INTERNATIONAL JOURNAL FOR NUMERICAL METHODS IN FLUIDS
Int. J. Numer. Meth. Fluids 2002; **40**:999–1007 (DOI: 10.1002/fld.386)

A Petrov–Galerkin method for flows in cavities: enclosure of aspect ratio 8

Sergey A. Suslov[1] and Samuel Paolucci[2,*,†]

[1] *Mathematics and Computing, University of Southern Queensland, Toowoomba, Queensland 4350, Australia*
[2] *Aerospace and Mechanical Engineering, University of Notre Dame, Notre Dame, ID 46556, U.S.A.*

SUMMARY

A Petrov–Galerkin method for computations of fully enclosed flows is developed. It makes use of divergence-free basis functions which also satisfy the boundary conditions for the velocity field. This allows the elimination of the unknown pressure. The computational procedure reduces to the solution of a system of non-linear first-order ordinary differential equations for the spectral expansion coefficients. We illustrate the effectiveness and accuracy of the method by solving the problem of the two-dimensional thermoconvective flow in a rectangular cavity of aspect ratio 8 at Rayleigh number 3.4×10^5. Copyright © 2002 John Wiley & Sons, Ltd.

KEY WORDS: convection; spectral methods; Petrov–Galerkin method; differentially heated cavity

1. INTRODUCTION

Spectral and, in particular, Galerkin-type methods are usually the first methods of choice when high accuracy of results is required in the solution of partial differential equations. But when a very large number of spectral modes is necessary to resolve the fine structures of the solution, the application of spectral methods might become computationally very expensive.

The proposed method (see Reference [1]) takes into account some of the properties of the flow and incorporates them into the construction of specific basis functions. This guarantees a faster convergence rate than obtained using conventional spectral methods.

2. PROBLEM FORMULATION

We consider the two-dimensional flow of a fluid with Prandtl number $Pr = \nu/\alpha = 0.71$ in a rectangular enclosure of aspect ratio $A = H/W = 8$ at the Rayleigh number $Ra = \beta g \Delta T W^3/(\alpha\nu) =$

* Correspondence to: S. Paolucci, Aerospace and Mechanical Engineering, University of Notre Dame, Notre Dame, ID 46556-5637, U.S.A.
† E-mail: paolucci.1@nd.edu

Received 31 December 2001
Revised 1 July 2002

Copyright © 2002 John Wiley & Sons, Ltd.

3.4×10^5 as introduced in Christon *et al.* [2]. The dimensionless governing equations, corresponding to conservations of mass, momentum and energy, under the Boussinesq approximation, are given by

$$\nabla \cdot \mathbf{u} = 0 \tag{1}$$

$$\frac{\partial \mathbf{u}}{\partial t} + \boldsymbol{\omega} \times \mathbf{u} = -\nabla P - \theta \mathbf{n} + \sqrt{\frac{Pr}{Ra}}\, \nabla^2 \mathbf{u} \tag{2}$$

$$\frac{\partial \theta}{\partial t} + \mathbf{u} \cdot \nabla \theta = \frac{1}{\sqrt{Pr\, Ra}} \nabla^2 \theta \tag{3}$$

where $\mathbf{u} = (u, v, 0)^{\mathrm{T}}$ is the velocity vector, $P = p + |\mathbf{u}|^2/2$ is the total pressure, and $\mathbf{n} = (0, -1, 0)^{\mathrm{T}}$ is the unit vector in the direction of gravity. Note that it is advantageous to introduce the vorticity vector $\boldsymbol{\omega} = (0, 0, \partial v/\partial x - \partial u/\partial y)^{\mathrm{T}}$ since in this case only two velocity derivatives enter the convective terms of the momentum equations instead of four.

Boundary conditions at the walls are

$$\mathbf{u} = \mathbf{0} \quad \text{at } x = 0, 1 \quad \text{and} \quad y = 0, A$$
$$\theta = \pm \tfrac{1}{2} \quad \text{at } x = 0, 1 \quad \text{and} \quad \frac{\partial \theta}{\partial y} = 0 \quad \text{at } y = 0, A \tag{4}$$

The initial conditions used are $\mathbf{u}_0 = \mathbf{0}$ and $\theta_0 = \frac{1}{2} - x$.

3. METHOD OF SOLUTION

To solve the system of Boussinesq equations (1)–(3) we require the spectral expansion bases to satisfy the following conditions: (1) the basis functions for velocity are divergence free, (2) the basis functions satisfy homogeneous boundary conditions, (3) the basis functions are complete in the space of continuous functions and (4) the system of approximate equations results in sparse matrices. These criteria lead to the following expansions for the unknown functions:

$$\begin{pmatrix} u \\ v \end{pmatrix} = \sum_{i=0}^{K} \sum_{j=0}^{L} C_{ij}(t) \begin{pmatrix} g_i(x) \cdot h_j'(y/A) \\ -A g_i'(x) \cdot h_j(y/A) \end{pmatrix}$$
$$\theta = \frac{1}{2} - x + \sum_{i=0}^{M} \sum_{j=0}^{N} D_{ij}(t) \cdot p_i(x) \cdot r_j(y/A) \tag{5}$$

with $C_{ij}(0) = D_{ij}(0) = 0$, where, upon using the transformations $\tilde{x} = 2x - 1$ and $\tilde{y} = 2y/A - 1$, we have for $i, j = 0, 1, 2, \ldots$

$$g_i(T(\tilde{x})) = T_i(\tilde{x}) - 2\left(\frac{i+2}{i+3}\right) T_{i+2}(\tilde{x}) + \left(\frac{i+1}{i+3}\right) T_{i+4}(\tilde{x})$$
$$h_j(T(\tilde{y})) = T_j(\tilde{y}) - 2\left(\frac{j+2}{j+3}\right) T_{j+2}(\tilde{y}) + \left(\frac{j+1}{j+3}\right) T_{j+4}(\tilde{y}) \tag{6}$$
$$p_i(T(\tilde{x})) = T_i(\tilde{x}) - T_{i+2}(\tilde{x}), \quad r_j(T(\tilde{y})) = T_j(\tilde{y}) - \left(\frac{j}{j+2}\right)^2 T_{j+2}(\tilde{y})$$

Copyright © 2002 John Wiley & Sons, Ltd.

Here $T_i(\tilde{x}) = \cos(i \arccos(\tilde{x}))$ are the Chebyshev polynomials of the first kind which are complete in the space of continuous functions on the interval $-1 \leqslant x \leqslant 1$.

Next we apply a Petrov–Galerkin procedure with the following test functions:

$$\mathbf{f}_{mn} = \begin{pmatrix} g_m(T(\tilde{x})/\sqrt{1-\tilde{x}^2}) \cdot h'_n(T(\tilde{y})/\sqrt{1-\tilde{y}^2}) \\ -A g'_m(T(\tilde{x})/\sqrt{1-\tilde{x}^2}) \cdot h_n(T(\tilde{y})/\sqrt{1-\tilde{y}^2}) \end{pmatrix}$$
$$q_{mn} = p_m(T(\tilde{x})/\sqrt{1-\tilde{x}^2}) \cdot r_n(T(\tilde{y})/\sqrt{1-\tilde{y}^2}) \tag{7}$$

These functions are chosen to satisfy the homogeneous boundary conditions and the divergence-free condition for the velocity test functions. The Chebyshev weights are introduced to take advantage of the orthogonality property of Chebyshev polynomials which guarantees the sparseness of the resulting matrices. The inner product of the vector momentum equation with the velocity test function $\mathbf{f}_{mn}$ is computed next. Note that for an arbitrary scalar function P and a divergence-free vector field $\mathbf{f}_{mn}$ which satisfies zero boundary conditions

$$\int_V \nabla P \cdot \mathbf{f}_{mn} \, \mathrm{d}V = -\int_V P \nabla \cdot \mathbf{f}_{mn} \, \mathrm{d}V + \int_S P \mathbf{f}_{mn} \, \mathrm{d}\mathbf{S} \equiv 0 \tag{8}$$

where V and S denote the volume and surface of the domain, respectively. Thus, the pressure is eliminated from the approximate equations identically. We also integrate the thermal energy equation over the volume after multiplying it by the test function q_{mn}. Thus, the Petrov–Galerkin procedure results in a system of *non-linear ordinary* differential equations for the spectral coefficients

$$\mathbf{S}\dot{\mathbf{X}} = \mathbf{A}\mathbf{X} + \mathbf{F}$$

where

$$\mathbf{X} = \begin{pmatrix} C \\ D \end{pmatrix}, \quad \mathbf{S} = \begin{pmatrix} S_{ff} & 0 \\ 0 & S_{qq} \end{pmatrix}$$
$$\mathbf{A} = \begin{pmatrix} \sqrt{Pr/Ra} A_{ff} & A_{fq} \\ A_{qf} & A_{qq}/\sqrt{PrRa} \end{pmatrix}, \quad \mathbf{F} = \begin{pmatrix} C^{\mathrm{T}} B_{fff} C + F_{ff} \\ C^{\mathrm{T}} B_{qfq} D \end{pmatrix} \tag{9}$$

Subscripts denote products of the basis functions participating in the Petrov–Galerkin integration. The coefficients A_{ff}, A_{fq}, A_{qf}, A_{qq}, B_{fff}, B_{qfq}, and F_{ff} consist of the inner products of Chebyshev polynomials which can be obtained analytically using integration by parts and the orthogonality property of Chebyshev polynomials.

By reordering the equations in the system the sparse matrices $\mathbf{S}$ and $\mathbf{A}$ are rearranged to block cyclic form [1]. The problem then is split into two parts coupled only through the non-linear terms in the vector $\mathbf{F}$. The first part corresponds naturally to the centro-symmetric solution, while the second part results in the centro-symmetry-breaking solution (see Reference [2] for definitions of symmetries). The full solution to the problem is a result of non-linear coupling between these two basic solutions. As follows from Equation (9) with the adopted (centro-symmetric) initial conditions $C_{ij} = D_{ij} = 0$, the only non-zero forcing term which affects the initial motionless conduction state is F_{ff} which traces back to the buoyancy term in the vertical momentum equation. Only one component of this vector corresponding to $i = j = 0$ is non-zero due to the special choice of the test functions and the orthogonality property of

Copyright © 2002 John Wiley & Sons, Ltd.

Chebyshev polynomials. This term, through its effect on the first linearly decoupled block, induces *only* a centro-symmetric solution such that

$$C_{ij}=0 \quad \text{if } i+j \quad \text{is } odd \quad \text{and} \quad D_{ij}=0 \quad \text{if } i+j \quad \text{is } even \tag{10}$$

The centro-symmetry-breaking component of the full solution then can develop only through feeding the truncation errors via the non-linear coupling in vector **F** into the second linearly decoupled block of the problem provided that the centro-symmetric solution is unstable with respect to symmetry-breaking disturbances *and* the truncation errors are indeed symmetry breaking. The natural splitting of the original problem into centro-symmetric and symmetry-breaking parts makes the linear stability analysis of these solutions very straightforward, although it will not be discussed here. The special form of matrices **A** and **F** also allows one to solve the problem by partitioning which would reduce the computational cost further, but this has not been done in the current computations. Further optimization of the solution procedure is possible if use is made of special sparse matrix solvers for multi-diagonal systems. At this point we have not focused our attention on this issue either, and subsequently have used a general sparse matrix package (YSMP).

The procedure just described is ideal if one is interested in the low-order dynamical system approximating the given problem. In this case all integrals, including triple products entering the non-linear terms, can be computed analytically and stored. Then the system of first-order ordinary differential equations with known constant coefficients can be solved using any appropriate initial value integration technique. When accurate solutions are required for higher values of Rayleigh numbers, the total number of spectral modes becomes large. The storage space required for triple product integrals in the two-dimensional case is proportional to N^6, where N is the number of modes in one direction (assumed equal in each direction). Thus memory limitations become extremely restrictive for the proposed method. Alternatively, a direct calculation of triple products at each time step makes the method extremely time consuming. Fortunately, this last difficulty can be resolved since the Chebyshev polynomial basis enables the use of fast Fourier transforms (FFTs) which require only $O(N^n \ln N)$ operations to evaluate nonlinear terms, where n is the spatial dimension of the problem. Algorithmically, we first find the expansions for $\boldsymbol{\omega}$, $\mathbf{u}$ and $\nabla\theta$ (the convection components) in terms of Chebyshev polynomials using recurrence differentiation formulae applied to the original expansion. Then we apply the inverse 2D FFT to find the values of $\boldsymbol{\omega}$, $\mathbf{u}$ and $\nabla\theta$ at $2N \times 2N$ Gauss–Lobatto collocation points. The choice of $2N$ collocation points in each direction allows us to retain full spectral accuracy since it leads to the exact evaluation of triple-product integrals. Lastly, we find values of non-linear terms in physical space using $O(N^2)$ operations and subsequently apply the forward 2D FFT to find the expansion of non-linear terms as Chebyshev series. Since the expansion of the trial functions in terms of Chebyshev polynomials is known, the integral evaluation reduces to the trivial use of orthogonality formulas.

To avoid the solution of the non-linear equations at each time step, and preserve the stability characteristics of implicit schemes as much as possible, we implement a semi-implicit time integration procedure combining the second order (implicit) Gear method for the linear part and the second-order (explicit) Adams–Bashforth method for the non-linear term. In the application to our matrix equation this becomes

$$(3\mathbf{S}-2\Delta t\mathbf{A})\mathbf{X}^{n+1}=\mathbf{S}(4\mathbf{X}^n-\mathbf{X}^{n-1})+2\Delta t(2\mathbf{F}^n-\mathbf{F}^{n-1}) \tag{11}$$

Copyright © 2002 John Wiley & Sons, Ltd.

If the time step Δt is fixed then the matrix on the left-hand side of Equation (11) can be inverted once and then the integration procedure reduces to matrix–vector multiplications which can be accomplished efficiently on parallel computers. The drawback of this is the significant increase of required computer memory as the inverse of the sparse matrix is much less sparse than the original one. For this reason, in the current realization of the algorithm, which ran on a serial computer, the memory saving option was used and the system of linear Equations (11) was solved at every time step using YSMP.

4. RESULTS

The computations were performed on a Sun UltraSPARC 30, Model 300 with a 296 MHz UltraSPARC-II CPU. The computational cost was approximately 3×10^{-4} s/time step/mode. Summaries of computed results are given in Tables I–VI and Figures 1 and 2. A major observation from the results is that the flow is periodic. Furthermore, because of the very high accuracy of the algorithm and centro-symmetry of the initial conditions, machine round-off errors are also centro-symmetric when $K = M = L = N$. Subsequently, the skewness parameter ε_{12} is identically zero whenever equal number of modes are used in the x and y directions. This is indicated in Table I. In Reference [1] we have shown that the centro-symmetry persists even in the chaotic regime occurring at higher Rayleigh numbers. However, this centro-symmetric chaotic flow is unstable to small symmetry breaking disturbances such

Table I. Numerical results at Point 1 ($x = 0.1810, y = 7.3700$) for $1000 \leqslant t \leqslant 1500$ using 34.61 samples/period and 692.24 time steps/period.

	$K = L = M = N = 50$			$K = M = 50,\ L = N = 70$		
	Required memory: 91 MB			Required memory: 155 MB		
Quantity	Average	PVA	Period	Average	PVA	Period
u	0.05653	0.05575	3.4012	0.05661	0.05243	3.4012
v	0.46190	0.07840	3.4012	0.45995	0.07309	3.4012
θ	0.26543	0.04352	3.4012	0.26784	0.04068	3.4012
ε_{12}	0	0	—	0.00466	0.01060	3.4012
ψ	−0.07367	0.00715	3.4012	−0.07323	0.00667	3.4012
ω	−2.36620	1.10125	3.4012	−2.35484	1.02932	3.4012
	$K = L = M = N = 70$			$K = M = 70,\ L = N = 100$		
	Required memory: 260 MB			Required memory: 483 MB		
Quantity	Average	PVA	Period	Average	PVA	Period
u	0.05638	0.05466	3.4012	0.05653	0.05310	3.4012
v	0.46195	0.07698	3.4012	0.46039	0.07419	3.4012
θ	0.26551	0.04260	3.4012	0.26728	0.04124	3.4012
ε_{12}	0	0	—	0.00352	0.00831	3.4012
ψ	−0.07372	0.00699	3.4012	−0.07334	0.006763	3.4012
ω	−2.37216	1.07503	3.4012	−2.35820	1.04320	3.4012

Copyright © 2002 John Wiley & Sons, Ltd.

Table II. Numerical results at Point 1 ($x = 0.1810, y = 7.3700$) for $1000 \leqslant t \leqslant 1500$ using 34.61 samples/period and 692.24 time steps/period; centro-symmetry is enforced.

	$K = M = 50,\ L = N = 70$			$K = M = 70,\ L = N = 100$		
	Required memory: 78 MB			Required memory: 245 MB		
Quantity	Average	PVA	Period	Average	PVA	Period
u	0.05638	0.05466	3.4012	0.05634	0.05467	3.4012
v	0.46200	0.07699	3.4012	0.46190	0.07700	3.4012
θ	0.26551	0.04260	3.4012	0.26552	0.04261	3.4012
ε_{12}	0	0	—	0	0	—
ψ	−0.07372	0.00699	3.4012	−0.07371	0.00700	3.4012
ω	−2.37216	1.07501	3.4012	−2.37171	1.07555	3.4012

Table III. Wall Nusselt numbers for $1000 \leqslant t \leqslant 1500$ using 34.61 samples/period and 692.24 time steps/period.

	$K = L = M = N = 50$			$K = M = 50,\ L = N = 70$		
Quantity	Average	PVA	Period	Average	PVA	Period
Nu_0	−4.57934	0.00730	3.4012	−4.56153	0.00670	3.4012
Nu_W	−4.57934	0.00730	3.4012	−4.59737	0.00750	3.4012
	$K = L = M = N = 70$			$K = M = 70,\ L = N = 100$		
Quantity	Average	PVA	Period	Average	PVA	Period
Nu_0	−4.57947	0.00710	3.4012	−4.56590	0.00680	3.4012
Nu_W	−4.57947	0.00710	3.4012	−4.59301	0.00740	3.4012

as those due to truncation errors occurring when different numbers of spectral modes are used in the x and y directions. Because of the natural partitioning between centro-symmetric and symmetry-breaking modes discussed in Reference [1], it is straightforward to enforce centro-symmetry even when different number of modes are used in the x and y directions. This is achieved by setting to zero the bottom half of all spectral coefficients and using only the top left quadrant in matrices **A** and **S**. The corresponding results are presented in Tables II, IV and VI. In the tables we also report the time-averaged values, peak-to-valley amplitudes and dominant periods computed from the results sampled between $t = 1000$ and 1500 using FFT. Note that these results change slightly for larger times when the number of modes is different in the x and y directions and centro-symmetry is not enforced. This indicates that the flow has not reached its steady state yet when symmetry breaking disturbances are allowed. It is also found that the periodic flow in the regime considered contains a second harmonic with the frequency twice the dominant one. Its amplitude decays with time. Although here we present only results for $Ra = 3.4 \times 10^5$ and $A = 8$ we have computed solutions for various other regimes. For example, a steady solution exists for relatively small values of the Rayleigh number and $A = 1$. It has been shown in Reference [1] that in this case the accuracy of our results is superior to that obtained by Le Quéré [3] using a pseudo-spectral Chebyshev

Copyright © 2002 John Wiley & Sons, Ltd.

Table IV. Wall Nusselt numbers for $1000 \leqslant t \leqslant 1500$ using 34.61 samples/period and 692.24 time steps/period; centro-symmetry is enforced.

	$K=M=50,\ L=N=70$			$K=M=70,\ L=N=100$		
Quantity	Average	PVA	Period	Average	PVA	Period
Nu_0	−4.57947	0.00708	3.4012	−4.57946	0.00708	3.4012
Nu_W	−4.57947	0.00708	3.4012	−4.57946	0.00708	3.4012

Table V. Square roots of global kinetic energy, $\hat{u}$, and enstrophy, $\hat{\omega}$, for $1000 \leqslant t \leqslant 1500$ using 34.61 samples/period and 692.24 time steps/period.

	$K=L=M=N=50$			$K=M=50,\ L=N=70$		
Quantity	Average	PVA	Period	Average	PVA	Period
$\hat{u}$	0.23954	4.07×10^{-5}	3.4012	0.23950	4.07×10^{-5}	3.4012
$\hat{\omega}$	3.01707	0.00326	3.4012	3.01716	0.00313	3.4012
	$K=L=M=N=70$			$K=M=70,\ L=N=100$		
Quantity	Average	PVA	Period	Average	PVA	Period
$\hat{u}$	0.23951	4.07×10^{-5}	3.4012	0.23950	4.07×10^{-5}	3.4012
$\hat{\omega}$	3.01710	0.00318	3.4012	3.01713	0.00318	3.4012

Table VI. Square roots of global kinetic energy, $\hat{u}$, and enstrophy, $\hat{\omega}$, for $1000 \leqslant t \leqslant 1500$ using 34.61 samples/period and 692.24 time steps/period; centro-symmetry is enforced.

	$K=M=50,\ L=N=70$			$K=M=70,\ L=N=100$		
Quantity	Average	PVA	Period	Average	PVA	Period
$\hat{u}$	0.23951	3.46×10^{-5}	3.4012	0.23951	3.46×10^{-5}	3.4012
$\hat{\omega}$	3.01710	0.00319	3.4012	3.01710	0.00319	3.4012

algorithm. With the current Petrov–Galerkin formulation we obtain the same accuracy using a substantially smaller total number of modes.

5. CONCLUSIONS

The developed Petrov–Galerkin method enables the efficient and spectrally accurate solution of incompressible fully enclosed flows using primitive variables. Pressure is eliminated identically from the system of equations by the special choice of the divergence-free basis satisfying homogeneous boundary conditions. Further reduction of the total number of unknown functions is obtained since the two velocity components are represented by one set of spectral coefficients. The even–odd decomposition of the modes is straightforward and allows to partition

Copyright © 2002 John Wiley & Sons, Ltd.

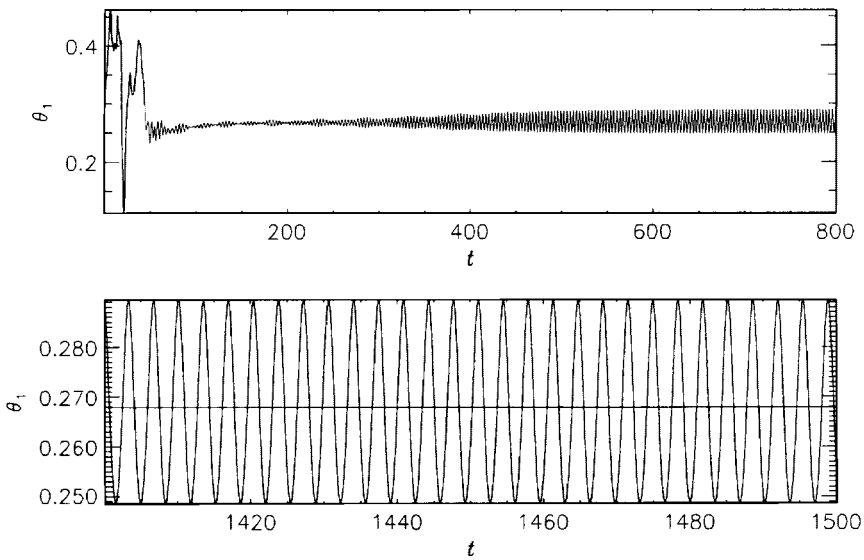

Figure 1. History of temperature at Point 1 ($x = 0.1810$, $y = 7.3700$), θ_1, with detail, for $K = M = 50$ and $L = N = 70$.

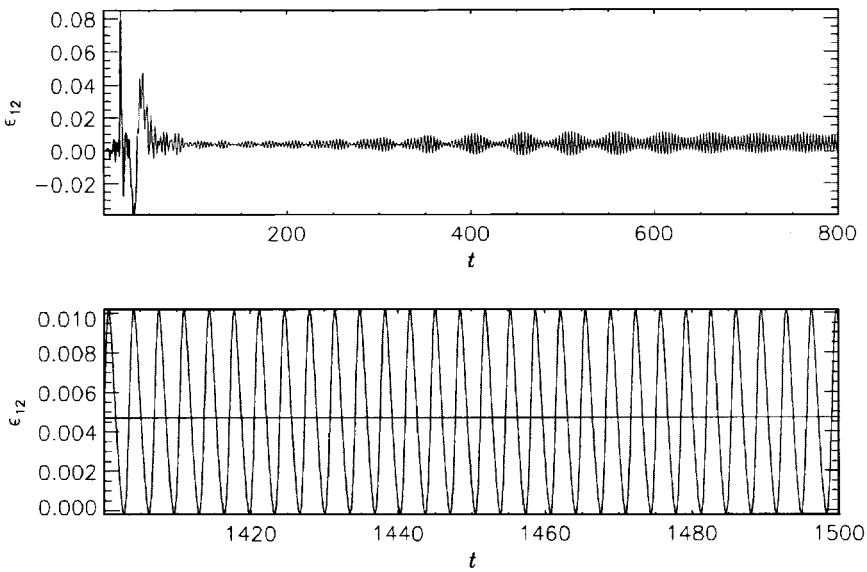

Figure 2. History of temperature skewness between Point 1 ($x = 0.1810$, $y = 7.3700$) and Point 2 at ($x = 0.8190$, $y = 0.6300$), ε_{12}, with detail, for $K = M = 50$ and $L = N = 70$.

Copyright © 2002 John Wiley & Sons, Ltd.

the problem leading to substantial computational savings. The numerical procedure is made very efficient by computing analytically and storing all necessary inner products and using FFTs for the explicit evaluation of non-linear terms. Further increase of the efficiency of the method can be achieved through the use of specialized sparse matrix solvers and straightforward parallelization of the algorithm which have not been implemented at this stage. Although not shown here, this technique is easily generalized to three dimensions resulting in even more substantial computer storage and computational time savings in comparison with other spectral techniques.

REFERENCES

1. Suslov SA, Paolucci S. A Petrov–Galerkin method for the direct simulation of fully enclosed flows. *Proceedings of the ASME Heat Transfer Division* 1996; **4**(HTD-335):39–46.
2. Christon MA, Gresho PM, Sutton SB. Computational predictability of natural convection flows in enclosures. *International Journal for Numerical Methods in Fluids* 2002; **40**:953–980.
3. Le Quéré P. Accurate solutions to the square thermally driven cavity at high Rayleigh number. *Computers and Fluids* 1991; **20**:29–41.

Copyright © 2002 John Wiley & Sons, Ltd.